Appl. Math. Inf. Sci. 6 No. 1S, 47S-58S (2012)

Applied Mathematics & Information Sciences
An International Journal

Multiresolution-Based Adaptive Simulation of Wave Equation

Hassan Yousefi[1], Asadollah Noorzad[1], Jamshid Farjoodi[1] and Mehdi Vahidi[1]
[1] School of Civil Engineering, Faculty of Engineering, University of Tehran, Tehran, Iran
Email Address: hyosefi@ut.ac.ir

Received: Received May 02, 2011; Revised July 25, 2011; Accepted September 12, 2011
Published online: 1 January 2012

Abstract: A modified wavelet-based adaptive-grid scheme is proposed for simulating elastic wave propagation in media with sharp transition of physical properties. The solution grid is adapted by interpolation wavelet; the wavelet transform is used as a tool to detect high-gradient zones. The cubic smoothing spline is employed as a postprocessor to remove spurious oscillations developed in the numerical solution of second order hyperbolic systems. The filtering procedure is directly done in the non-uniform grid, an ill-posed problem. Smoothing splines are indeed a kind of Tikhonov regulization method; hence the smoothing results are stable and reliable. This smoothing method works satisfactory in irregular grid points. Finally some 2D wave propagation problems are simulated to demonstrate the efficiency of the proposed method.

Keywords: Adaptive Wavelet; Smoothing Spline; Tikhonov Regularization; Hyperbolic Systems; Wave Equation

1 Introduction

Grid-based adaptive wavelet methods have successfully been developed for Partial Differential Equations (PDEs) solutions which contain steep moving fronts or sharp transitions in small zones, e.g. [1-4]. In these methods, the wavelet transforms are used to detect highly non-uniform spatial behaviors and corresponding zones. The wavelet transforms act actually as a mathematical microscope, investigating a data locally in different resolutions. Wavelets can adequately resolve different scales. They use high resolutions only near sharp transition regions, while moderate resolutions are applied in the regions with smooth and slow varying behaviors. These schemes have mostly been improved for elliptic and parabolic PDEs [1-3]. The hyperbolic PDEs, on the other hand, could not be simulated by common adaptive procedures, i.e., incorporating wavelet-based grid adaptation procedure with other common numerical schemes for solving PDEs (e.g., common finite-difference or collocation method). In comparison with the elliptic and parabolic cases, the hyperbolic systems show no inherent dissipation. This feature ends to develop non-physical oscillations and instability in the both solution and corresponding adaptation procedure. Regarding second order hyperbolic PDEs, some common approaches used to remedy above mentioned drawbacks, are: 1) dissipative time integration schemes [5]; 2) spatial smoothing (or spectral filtering). However, using such approaches do not necessarily lead to the smoothest possible solutions, essential for proper adaptation procedure. Here a post-processing approach is comprised with common wavelet-based grid adaptation procedure to remove spurious oscillations. The smoothing method is the cubic smoothing spline, a kind of Tikhonov regularization method [6]. The method is stable, fast [7] and not sensitive to noise ratio [8]. This scheme of smoothing can directly be used in irregular grid points. Smoothing spline of $2m-1$ degree has continuous derivations up to $2m-2$ [th] [6].

Regarding smoothness and error in estimation, one of the common numerical approaches, the generalized-α dissipative time integration scheme,

is compared with the proposed method by a bench-mark problem. It is a wave propagation problem containing nearly discontinuous propagating front. There, the trade-off between smoothness and error in estimation is visually studied by the L-curve method [9].

Here, the spatial derivatives are directly approximated in the irregular grid points. The interpolation is locally done by five point based Lagrange polynomial. Anti-symmetric end padding method is used to reduce edge effects from the derivatives in 2D simulations [4]. This modification leads to zero second derivatives at the end points. Hence, the moving fronts propagate with constant speed.

Finally some wave equations are simulated; especially problems include abrupt transition in material properties.

2 Multiresolution-based Grid Adaptation

2-1 Dubuc-Deslauriers Interpolating Wavelets

Here, Dubuc-Deslauriers (D-D) interpolating wavelets are used for grid adaptation [1,2,10]. Using such family leads to a simple and straightforward algorithm (having physical meaning) for wavelet coefficient calculation. Also for reconstruct a function of constant accuracy; this family uses minimal grid points. This is a preferable feature in grid adaptation, since in adaptation a data, it is assumed that grid points in level resolution j (points with spatial distance $1/2^j$ to each other) are locally correlated; this assumption may not be true for points of large distance from each other.

In the following this family of interpolating wavelet is reviewed. In general, if $\phi_0(x)$ is a compact support orthonormal scaling function, then its autocorrelation, $\phi(x)$ is an interpolating scaling function [10]; Thereby, properties of function $\phi(x)$ are inherent from $\phi_0(x)$. For example, auto-correlations of Haar scaling function and Daubechies scaling function of order M (having M vanishing moments) lead to interpolating Schauder scaling function and the D-D scaling function of order $2M-1$, respectively; the latter one has the support size: $Supp(\phi)=[-2M+1,2M-1]$ [10].

To obtain a perfect reconstruction, Donoho [11] defines the D-D wavelet function as $\psi(x)=\phi(2x-1)$. This wavelet, hence, satisfies the interpolation feature [10].

2-2 Multiresolution Analysis and Adaptation of 1D Grid

Several points are assumed in a dyadic grid and mentioned as follows:

$$V_j=\{x_{j,k}\in R: x_{j,k}=k/2^j\};\ j\in Z; k\in\{0,1,\cdots,2^j\} \quad (2.1)$$

where, j is the resolution level and k is spatial position. Such definition of dyadic grid points V_j is ended to the $x_{j-1,k}=x_{j,2k}$ condition and the multiresolution representation core: i.e., $V_{j-1}\subset V_j$.

A function $f(x)$, defined in $V_{J_{\max}}$, is assumed (i.e., $x\in V_{J_{\max}}$). Regarding the multi-resolution representation, it is possible to show that any continuous function $f(x)$ can be described as follows [1, 10]:

$$f(x)=\sum_{l=0}^{2^{J_{\min}}} c_{J_{\min},l}.\varphi_{J_{\min},l}(x)+\sum_{j=J_{\min}}^{J_{\max}-1}\sum_{n=0}^{2^j} d_{j,n}.\psi_{j,n}(x) \quad (2.2)$$

where, $\varphi(x)$ and $\psi(x)$ are scaling and wavelet functions, respectively; $\varphi_{j,k}(x)$ and $\psi_{j,k}(x)$ are the dilated and shifted versions of $\varphi(x)$ and $\psi(x)$, respectively, i.e.: $\varphi_{j,k}(x)=\varphi(2^j x-k)$, and $\psi_{j,k}(x)=\psi(2^j x-k)$. $c_{j,k}$ and $d_{j,k}$ are approximation and detail coefficients, respectively. These coefficients can generally be obtained by projection method by considering orthogonally or bi-orthogonally feature of wavelet families [10].

Regarding interpolation properties of D-D families, alternative simple procedure can be provided for $c_{J_{\min},k}$ and $d_{j,n}$ evaluations. The approximation coefficients are equal to sampled values of $f(x)$ at points $x_{J_{\min},k}$ (the points included in $V_{J_{\min}}$), i.e., $c_{J_{\min},l}=f(x_{J_{\min},l})$ [1,10], by considering the interpolating property.

The detail coefficients are evaluated using multi-resolution analysis and interpolation feature of wavelet function. Namely, due to the properties $V_{J_{\min}}\subset\cdots\subset V_j\subset V_{j+1}\subset\cdots\subset V_{J_{\max}}$ and $\varphi(n-k)=\delta_{n,k}$. Due to the fact that $Pf_j(x_{j,k})=f(x_{j,k})$, and $x_{j,k}=x_{j+1,2k}$; then it is clear that:

$$Pf_j(x_{j,k})=Pf_{j+1}(x_{j+1,2k})=f(x_{j+1,2k}).$$

where $Pf_j=\sum_{l=0}^{2^j} c_{j,l}.\varphi_{j,l}(x)$ shows the approximation of $f(x)$, defined in grid points V_j. For odd-numbered grid points $x_{j+1,2k+1}$ including in V_{j+1}, in general, $pf_{j+1}(x_{j+1,2k+1})\neq f(x_{j+1,2k+1})$. The differences between $f(x_{j+1,2k+1})$ and $Pf_{j+1}(x_{j+1,2k+1})$ are measured

as the magnitudes of detail coefficients. This difference measures locally the smoothness of the function at point $x_{j+1,2k+1}$. The values of $Pf_{j+1}(x_{j+1,2k+1})$ are estimated by locally Lagrange interpolation by the known even-numbered grid points in V_{j+1} (i.e., the points belong to V_j and V_{j+1}). The interpolation is done by $2M$ (for the D-D wavelet family of order $2M-1$) most neighbor points in the vicinity of $x_{j+1,2k+1}$; the points are: $\{x_{j+1,2k-2n}\}$ $n\in\{-M+1,-M+2,\cdots,M\}$. Finally the coefficients $d_{j,n}$ are evaluated as [1]:

$$d_{j,n}=f(x_{j+1,2n+1})-Pf_{j+1}(x_{j+1,2n+1}) \qquad (2.3)$$

For adaptation a grid, at first a predefined threshold ε is assumed, then in each level of resolution $j\in\{J_{\min},J_{\min}+1,\cdots,J_{\max}-1\}$ where $f(x)\in V_{J_{\max}}$, odd-numbered points $x_{j+1,2n+1}$ are omitted from the calculating grid points, if corresponding $d_{j,n}$ satisfy the condition $d_{j,n}<\varepsilon$. It should be mentioned that wavelet coefficients and grid points have one-to-one correspondence. This relationship is illustrated if Fig. 1(a) for a grid of length 2^7+1. In this figure, solid points represent distribution of grid points at different levels of resolution. There, points at levels 3-6 are wavelet coefficient locations; the coefficients in level j span j^{th} detail space. Besides, points in the first level show locations of scale coefficients, which span the smooth approximation space; these points are also known as the base-grid (back ground) points. In brief, each point only belongs to a specific level of resolution. In Fig. 2, lines emphasis that the points have dyadic form.

In the following a test function $f(x)=Exp(-2000(x-0.5)^2)$ is selected, where $x\in[0,1]$. The function is illustrated in Fig. 1(b) with gray line. It is assumed that $f(x)=f_{J_{\max}=7}(x)$ (i.e., the sampling step is $1/2^7$ or number of grid points is $N_x=2^7+1$). The discrete data is adapted by the D-D wavelet of order 3 ($M=2$) with predefined threshold $\varepsilon=10^{-5}$. The adapted grid is shown in Fig. 2(b) by solid point. In the Fig. 1(c), the dyadic grid point locations and adapted points corresponding to $f(x)$ are shown respectively by solid points and empty circles. There, j denotes the level of resolution. The results indicate that the adapted points are correctly concentrated in high gradient zones.

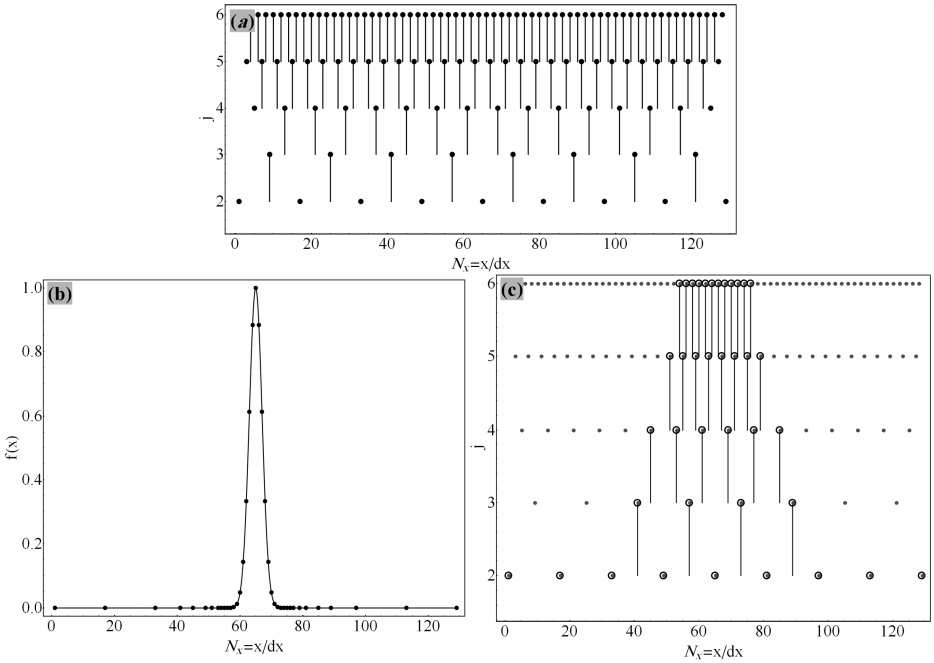

Fig. 1. dyadic grid points and corresponding adapted points; a) distribution of dyadic grid points in the different levels of resolution; b) a test function $f(x)=Exp(-2000(x-0.5)^2)$ and corresponding adapted grid points, (c) dyadic grid points at different levels of resolution (solid point) and adapted grid points (circles). In figures (b-c), it is assumed that: $\varepsilon=10^{-5}$.

The aforementioned procedure is applied for data of infinite length. For finite data the boundary wavelets, introduced by Donoho [11], could be used in the vicinity of edge points.

The above mentioned transform and reduction techniques can easily be extended to 2D grid points based on 1D algorithm [2].

For resolution of PDE in vector system, the previous procedure is modified to reflect the behavior of the solutions in all equations. Namely, the resultant adapted grid is simply the superposition of all adapted grids.

3 Tikhonov Regularization and Smoothing Splines

A problem is called ill-posed if it violates one of the following conditions:

I. The solution exists,

II. The solution is unique,

III. The solution is stable; namely, any perturbation of coefficients, parameters, initial or boundary conditions cause a little change in answers [12].

Many ill-posed problems could be occurred in numerical computations; some of which are: evaluation of derivatives in noisy data; estimation of a data and corresponding derivatives in irregularly sampled data.

Indeed, ill-posed problems have certain solutions; however, they should be obtained with especial treatments. The solutions of these problems are captured by regularization schemes. In these methods extra information are used to estimate real answers. By using the regularization methods, ill-posed problems are replaced with nearly well-posed ones. In the famous Tikhonov regularization method, the regulated (stable) answer is obtained by minimizing a functional which is a linear combination of residual norm ($\rho(y)^2 = \|y - y_{estimate}\|_2^2$) and additional information ($\Omega(y)^2$), where y is the real solution, and $y_{estimate}$ is the estimated one. In the Tikhonov regularization scheme the functional which must be minimized is [8,10]: $\rho(y)^2 + \lambda \times \Omega(y)^2 = \min_y$

where λ $(0 \le \lambda < \infty)$ is the regularization (smoothing) parameter which controls trade-off between smoothing and error in estimation [9, 12]. To investigate this relationship, residual norms in estimations are presented against regularization (semi) norms in Log-Log scales; x-axis and y-axis correspond to residual and regularization norms respectively. This visual method is known as the L-curve scheme [9].

If it is assumed that $\Omega(f)^2 = \int \left| (d^m f(x)/dx^m) \right|^2 dx$, then the method leads to the smoothing spline of order $2m-1$ [4]. To confine regularization parameter range between 0 and 1, it can be assumed that: $\lambda = (1-p)/p$, where $0 \le p \le 1$; in general, smaller p values leads to smoother estimations. To minimize curvature in estimation, here, cubic smoothing spline is used, i.e., $m = 2$ [4].

4 Wavelet-based Adaptive-grid Method for Solving PDEs

At the time step ($t = t_n$), if the solution of PDE is $f(x,t)$, then the procedure for PDE wavelet-based adaptive solution is:

1) Determining the grids, adapted by adaptive wavelet transform, using $f(x, t_{n-1})$ (step $n-1$). The values of points without $f(x, t_{n-1})$, are obtained by locally interpolation (for example, by cubic spline method);

2) Computing the spatial derivatives in the adapted grid using local Lagrange interpolation scheme, improved by anti-symmetric end padding method [4]. In this regard, extra non-physical fluctuations, deduced by one sided derivatives, are reduced. Here, five points are locally chosen to calculate derivatives and therefore a high-order numerical scheme is achieved;

3) Discretizing PDEs in spatial domain first, and then solving semi-discrete systems. The standard time-stepping methods such as Runge-Kutta schemes can be used to solve ODEs at the time $t = t_n$;

4) Denoising the spurious oscillations directly performed in non-uniform grid by smoothing splines;

5) Repeating the steps from the beginning.

For 1-D data of length n, smoothing spline of $2m-1$ degree, needs $m^2.n$ operations [7], and a wavelet transform (employing pyramidal algorithm)

uses n operations. Therefore both procedures are both fast and effective enough. However for cost effective simulation, the grid is adapted after several time steps (e.g. 10-20 steps) based on the velocity of moving fronts. In this case, the moving fronts are properly captured by adding some extra points to the fronts of adapted grid at each resolution level (e.g., 1 or 2 points to each end at each level).

5 Benchmark Problem

In the following, performance of the proposed method and another common approach, generalized-α dissipative time integration method [5], are compared with respect to their smoothness and accuracy properties. The considered problem is wave propagation in an elastic unit length rod, containing a nearly discontinuous solution is considered. It is assumed that, the rod is only subjected to an imposed initial displacement $u_0(x)$ (i.e., $\dot{u}_0(x)=0$); the displacement is:

$$u_0(x)=\begin{cases}\{x-(0.4-d)\}/d; & 0.4-d\le x\le 0.4\\ 1; & 0.4<x<0.6\\ 1-\{(x-(0.6+d))/d\}; & 0.6\le x\le 0.6+d\\ 0; & \textit{else where}\end{cases} \qquad (5.1)$$

where the wave velocity in rod is $c=1$.

The common approach is the finite element formulation employing dissipative time integration algorithm to filter high frequency component of solutions. In this temporal integration, symbols α, β and γ are free parameters which control the stability and numerical dissipation of the algorithm. For case $\gamma>0.5$ numerical dissipation is presented; and for $\beta\ge 0.25(\gamma+0.5)^2$ the mentioned algorithm is unconditionally stable [5]. In simulations, it is assumed that: $\gamma\in\{0.52,0.6,0.7\}$ and $\beta=0.25(\gamma+0.5)^2$. The assumed α range for each γ value is: 1) for $\gamma=0.52$, $0.15\alpha_0\le\alpha\le 0.001\alpha_0$; 2) for $\gamma=0.6$, $1.5\alpha_0\le\alpha\le 0.5\alpha_0$; 3) for $\gamma=0.7$, $1.55\alpha_0\le\alpha\le 0.3\alpha_0$; where $\alpha_0=-0.0683$.

Here 257 grid points (for the proposed scheme) and 257 finite elements of linear shape functions are utilized in simulations. The performance of the two aforementioned methods, with respect to smoothness and error in estimation, is presented in Fig. 2 at $t=0.2$. There, in case of finite element based simulation, another temporal time integration scheme, 4th order Runge-Kutta method is also studied (see Fig. 2). The results show that for a distinct error in estimation, smoothing spline based method leads to the smoothest results.

5 Numerical Examples

The following examples are to study the effectiveness of the proposed method concerning some phenomena in elastodynamic problems. The wave propagation phenomena (single or systems of PDEs) are studied in three cases: rectangle membrane with four fixed sides, two-layered media (fluid-solid configuration), and an infinite-media with fluid-filled crack.

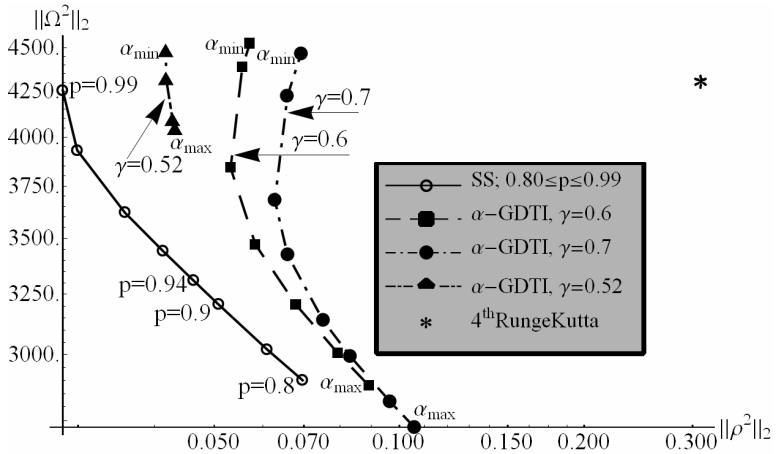

Fig. 2. Representation of smoothness ($\|\Omega^2\|_2$) against solution error ($\|\rho^2\|_2$) for the smoothing spline (SS) based method (the proposed scheme), implicit α - generalized dissipative time integration based method (α -GDTI), and 4th order Runge-Kutta based scheme.

Regarding using multiresolution adaptive algorithm, the simulation of wave-fields can properly be performed in the media especially with localized sharp transition of physical properties.

The examples of such media are fluid-solid configurations and the ones with fluid-filled cracks. In fact, to be analyzed by traditional uniform grid-based methods, these media show major challenges.

The main assumptions are: 1- applying D-D interpolating wavelet of order 3; 2- decomposing the grid (sampled at $1/2^8$ spatial step in the finest resolution) in three levels; 3- repeating re-adaptation and smoothing processes every ten time steps.

Example 1

To investigate smoothing and anti-symmetric end-padding effects, in the following, a tensioned square membrane subjected to an initial imposed deformation is considered. The equation of motion is:

$$\begin{aligned} &PDE \quad c_0^2\left(u_{,xx}+u_{,zz}\right)=u_{,tt},\ \Omega\in[0,1]\times[0,1] \quad 0\le t<\infty \\ &ICs \quad u(x,z,0)=U(x,z),\ \dot{u}(x,z,0)=0 \\ &BCs \quad u(0,z,t)=u(1,z,t)=0;\quad ,u(x,0,t)=u(x,1,t)=0 \end{aligned} \tag{6.1}$$

where the initial deformation is: $U(x,z)=\exp(-500\{(x-0.5)^2+(z-0.5)^2\})$. The evaluating assumptions are: $c_0=1$, $\varepsilon=10^{-5}$, and $dt=0.00015$.

Four numerical solutions are carried out using different assumptions; they are:

I. Simulating without using smoothing technique ($p=1$) while utilizing end-padding scheme (anti-symmetric end padding one),

II. Using both slightly amount of smoothing ($p=0.98$) and end-padding scheme,

III. Utilizing enough amount of smoothing ($p=0.8$), while do not using end-padding method,

IV. Employing both enough amount of smoothing ($p=0.8$), and end-padding scheme.

For case I, the solution at time 0.439 is shown in Fig. 3(a); Fig. 3(b) is the zoomed in solution at middle media (where waves propagated outward). It is obvious that small spurious oscillations still remain in such zones.

Considering assumptions I-IV, the corresponding adapted grids are illustrated in Fig. 4 at time 0.35. There, Fig. 4(a) is the solution and Figs. 4(b) through 4(e) correspond to assumptions I to IV, respectively. It is clear that due to non-physical oscillations in case $p=1$, the adaptation is failed (Fig. 4(b)).

Existence of even small amount of smoothing, significantly improves the adaptation ((Figs. 4(c) & 4(d)). The enhanced adaptation procedure could be captured by using end-padding methods ((Fig. 4(e)).

Example 2

In this example, the wave-fields are presented in two-layered media with sharp transition of physical properties in fluid-solid configurations. The numerical methods which do not increase the number of grid points around the interface have difficulties with the problems of fluid-solid contacts. In such problems, the speeds of elastic waves are largely different. The incident waves, P or S, coming from inside solid layer source can be reflected from interface in the form of P and S waves. It means that the incident P wave is reflected as PPr & PSr and the incident SV wave as SPr & SSr. Where, Pr and Sr are the reflected P and S waves, respectively. However, only P waves are transmitted to the fluid layer in the form of PPt & SPt waves, for incident P and SV waves, respectively; where, Pt is the transmitted P wave. The schematic shape of the media and the description of fluid-solid configuration are illustrated in Fig. 5.

In the numerical simulation it is assumed that: $p=0.8$ and $\varepsilon=0.5\times10^{-5}$, furthermore, the medium is subjected to an initial imposed deformation, at point S in the solid layer.

This deformation is shown by:

$$u_z(x,z,t=0)=\exp(-500((x-0.35)^2+(z-0.525)^2)).$$

Here, the absorbing boundary condition is considered explicitly for simulation infinite boundaries. Therefore, the wave equation is modified by a damping term $Q(x,z)\dot{u}(x,z,t)$ where, $Q(x,z)$ is an attenuation factor. This factor is zero in computation domain and increases gradually approaching to the artificial boundaries [13]. Consequently, the waves incoming towards these boundaries are gradually diminished.

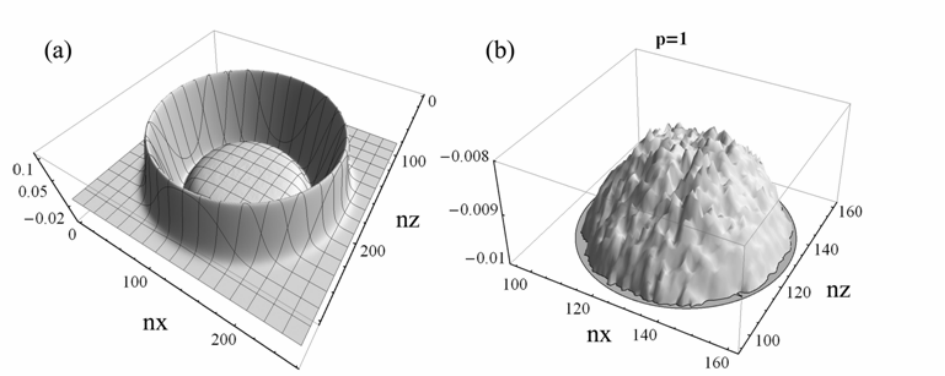

Fig. 3. The solution and corresponding spurious oscillations at time 0.439, a) the solution, b) the zoomed in solution.

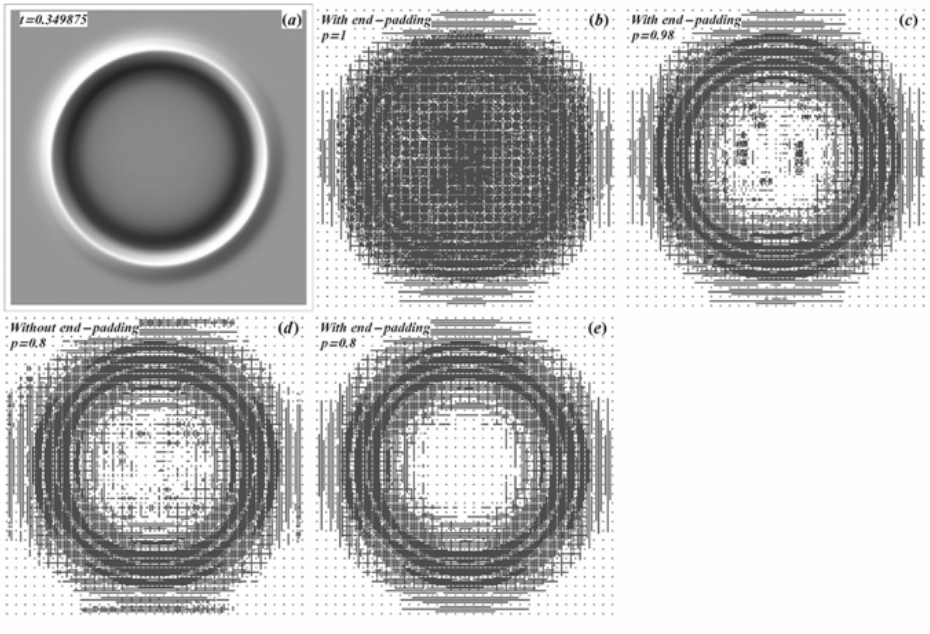

Fig. 4. The solution and corresponding adapted grid points for different assumptions, a) the numerical solution, b-e) adapted grids of Figs. (b) to (e) correspond to assumptions I through IV, respectively.

The mentioned above modification, performed for P-SV wave equations is as follows:

$$\left((\lambda+2\mu)u_{x,xx}+\mu u_{x,zz}\right)+\left((\lambda+\mu)u_{z,xz}\right)=\rho(\ddot{u}_x+Q(x,z).\dot{u}_x)$$
$$\left((\lambda+2\mu)u_{z,zz}+\mu u_{z,xx}\right)+\left((\lambda+\mu)u_{x,xz}\right)=\rho(\ddot{u}_z+Q(x,z).\dot{u}_z) \quad (6.2)$$

where $a_x=a_z=30$, and $b_x=-110, b_z=-70$.

Here, it is assumed that:

$$Q=a_x(e^{b_x.x^2}+e^{b_x.(1-x)^2})+a_z(e^{b_z.(1-z)^2}),$$

The snapshots of solutions u_x and u_z are shown in Figs. 6 and 7, respectively.

In each figure, the results are obtained at 0.036, 0.1, 0.168, and 0.2 sec, illustrated in figures (a) through (f), respectively. The reflected and transmitted waves are marked in Fig. 7 for studying the interface effects.

The adapted grid points, obtained by components u_x and u_z are illustrated in Fig. 8. It is clear that the grid points are properly concentrated in the high gradient and fluid-solid contact zones.

Example 3

Here, the wave propagation is modeled in a medium with high and abrupt variation in its physical parameters.

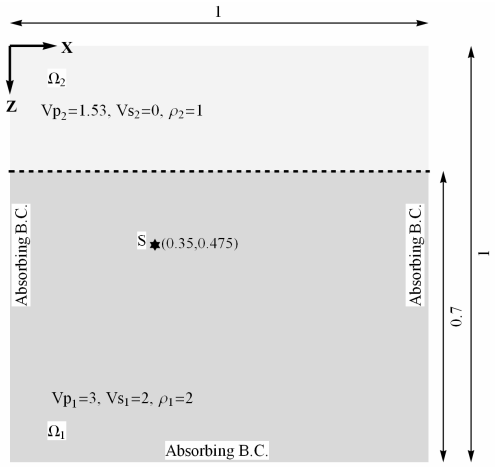

Fig. 5. Schematic plot of two layered-medium. Initial imposed deformation is subjected at point S.

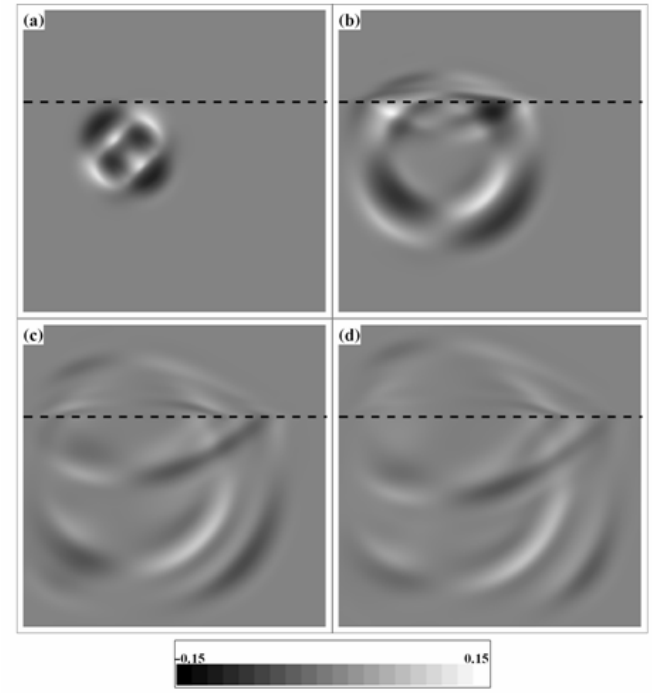

Fig. 6. Snapshots of solution u_x at 0.036, 0.1, 0.168, and 0.2 sec., illustrated in figures (a) through (d), respectively.

The medium has a narrow fluid-filled crack. Each P or S incident waves are reflected and transmitted as explained in example 2.

However, the P wave is diffracted from the crack into the solid media in the form of PPd & PSd. Where, Pd and Sd are the diffracted P and S waves, respectively.

The schematic shape of media along with the description of fluid-solid configuration is illustrated in Fig. 9.

In the numerical simulation it is assumed that: $p = 0.8, \alpha = 0$ and $\varepsilon = 10^{-5}$, furthermore, the medium is subjected to an initial imposed deformation at the point S in the solid layer. This deformation is shown by:

$$u_z(x, z, t = 0) = \exp(-500((x - 0.4)^2 + (z - 0.75)^2))$$

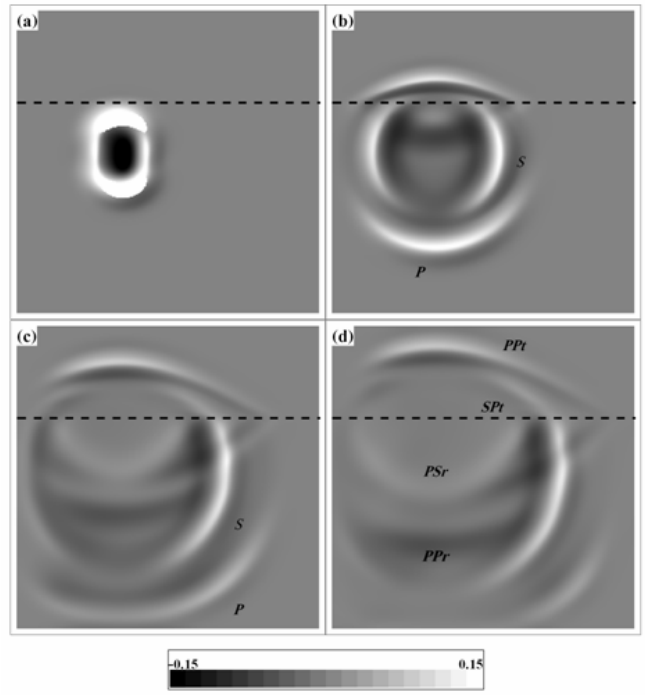

Fig. 7. Snapshots of solution u_z at 0.036, 0.1, 0.168, and 0.2 sec., illustrated in figures (a) through (d), respectively.

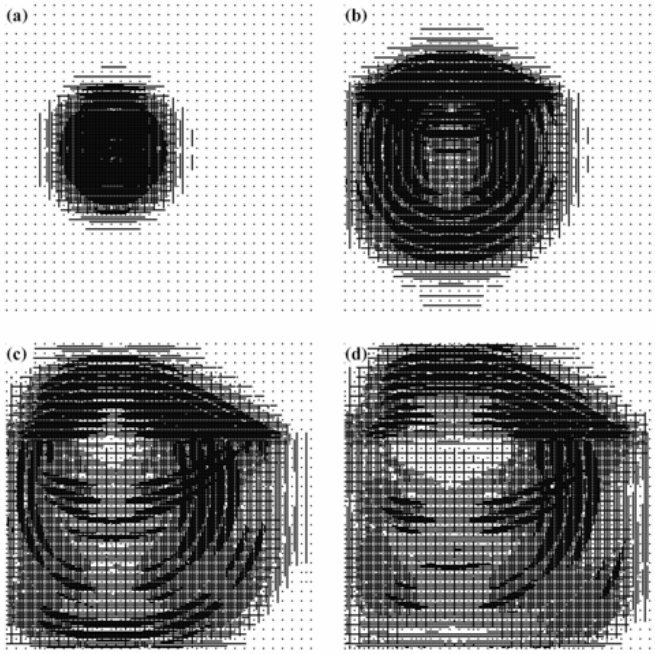

Fig. 8. Snapshots of adapted grids correspond to the solutions u_x and u_z at 0.036, 0.1, 0.168 and 0.2 sec., illustrated in figures (a) through (d), respectively.

The snapshots of u_x and u_z are shown in Figs. 10 and 11, respectively. In each figure, the solutions

are obtained at 0.036, 0.1, 0.168, and 0.2 sec, illustrated in figures (a) through (d), respectively. The adapted grids, corresponded to the above mentioned figures, are illustrated in Fig. 12. According to the results, the adapted grids are properly concentrated both in high gradient zones and in the vicinity of fluid-filled crack.

6 Conclusion

In this work, some wave propagation problems are simulated via wavelet-based adaptive grid method. The results show that the improved method can properly concentrate adapted points in the vicinity of both propagating fronts and zones containing abrupt changing in physical properties.

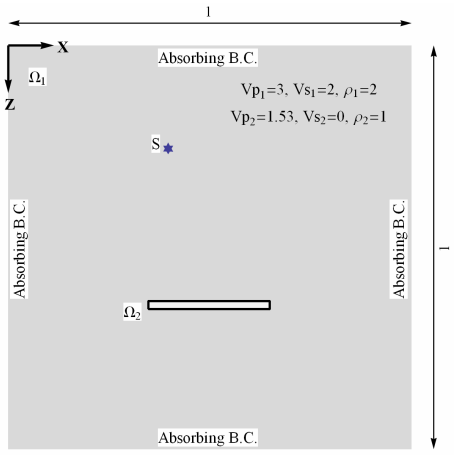

Fig. 9. Schematic shape of a fluid-filled crack in infinite media. Initial imposed deformation is subjected at point S.

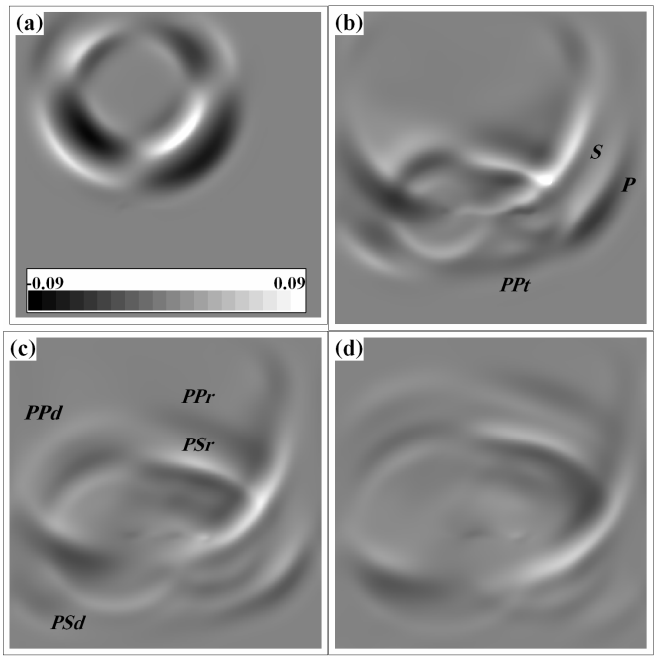

Fig. 10. Snapshots of solution u_x at 0.0737, 0.143, 0.175, and 0.205 sec., illustrated in figures (a) through (d), respectively.

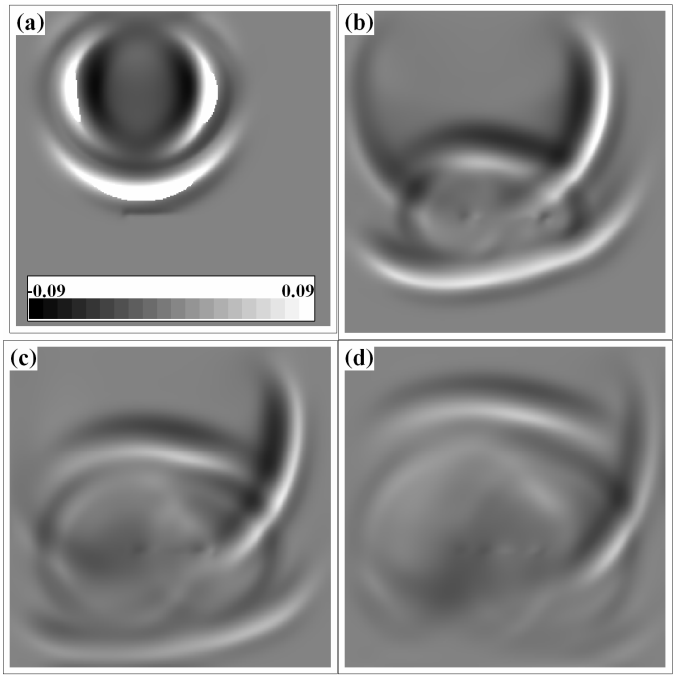

Fig. 11. Snapshots of solution u_z at 0.0737, 0.143, 0.175 and 0.205 sec., illustrated in figures (a) through (d), respectively.

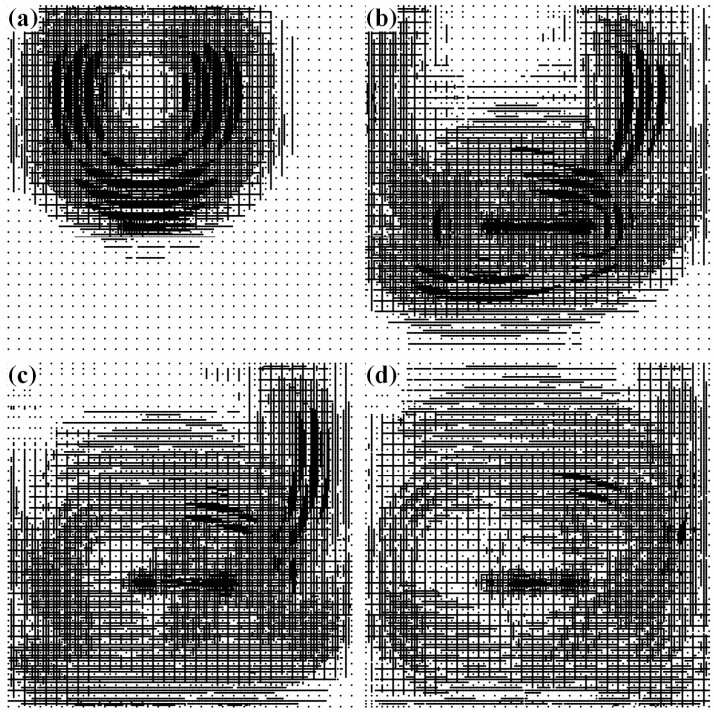

Fig. 12. Snapshots of adapted grids correspond to the solutions u_x and u_z at 0.0737, 0.143, 0.175 and 0.205 sec., illustrated in figures (a) through (d), respectively.

In addition, the results indicate that using both smoothing method and anti-symmetric end-padding scheme leads to a proper adaptation procedure. Finally, it is shown that the proposed method leads to the smoothest possible solution for a distinct error in estimation. This is because a Tikhonov based regularization scheme is utilized to remove spurious oscillations from numerical simulations.

References

[1] Cruz P., Mendes A., Magalhães F.D. Wavelet-based adaptive grid method for the resolution of nonlinear PDEs. AIChE Journal. Vol. 48, No. 4, (2002), 774-785.

[2] Santos J.C., Cruz P., Alves M.A., Oliveira P.J., Magalhães F.D., Mendes A. Adaptive multiresolution approach for two-dimensional PDEs. Comput. Meth. Appl. Mech. Eng. Vol. 193, No. 3, (2004), 405-425.

[3] Vasilyev O.V., Kevlahan N.K.R. An adaptive multilevel wavelet collocation method for elliptic problems. J. Comput. Phys. Vol. 206, No. 2, (2005), 412-431.

[4] Yousefi H., Noorzad A., Farjoodi J. Simulating 2D waves propagation in elastic solid media using wavelet based adaptive method. J. Sci. Comput. Vol. 42, (2010), 404-425.

[5] Hilber H.M., Hughes T.J.R., Taylor R.L. Improved numerical dissipation for time integration algorithms in structural dynamics. Earthq. Eng. Struct. Dyn. Vol. 5, (1977), 283-292.

[6] Unser M. Splines: a perfect fit for signal/image processing. IEEE Signal Process. Mag. Vol. 16, No.6, (1999), 22-38.

[7] Hutchinson M.F., de Hoog F.R. Smoothing noisy data with spline functions. Numer. Math. Vol. 47, No 1, (1985), 99-106.

[8] Ragozin D.L. Error bounds for derivative estimates based on spline smoothing of exact or noisy data. J. Approx. Theory. Vol 37, (1983), 335-355.

[9] Hansen P.Ch., Rank-Deficient and Discrete Ill-posed Problems. SIAM, Philadelphia, 1998.

[10] Mallet S. A Wavelet Tour of Signal Processing. Academic Press, San Diego, 1998.

[11] Donoho D.L. Interpolating wavelet transforms. Technical Report 408, Department of Statistics, Stanford University, 1992.

[12] Petrov Yu.P., Sizikov V.S. Well-posed, Ill-posed, and Intermediate Problems with Applications. VSP, Netherlands, 2005.

[13] Sochacki J., Kubichek R., George J., Fletcher W.R., Smiths S. On absorbing boundary conditions and surface waves. Geophysics. Vol. 52, No. 1, (1987), 60-71.

Hassan Yousefi received the PhD degree in earthquake engineering from University of Tehran, Iran. He is currently a research assistant in research center of school of civil engineering, University of Tehran. His research interests are in the areas of wave propagation, regularization schemes, wavelet theory, image processing and signal processing, hyosefi@ut.ac.ir.

Asadollah Noorzad received the PhD degree in earthquake engineering from University of Tokyo, Japan. He is currently a Professor in school of civil engineering, university of Tehran, Iran. Also, he is the head of research center in civil engineering, University of Tehran. His research interests are signal processing, applied mathematics in engineering seismology, soil structures interaction, and wave propagation, noorzad@ut.ac.ir.

Jamshid Farjoodi received the PhD degree in earthquake engineering from University of Tokyo, Japan. He is currently a Professor in school of civil engineering, university of Tehran, Iran. His research interests are wave propagation, random vibration, nonlinear dynamic analysis and seismic risk analysis, jfarjood@ut.ac.ir.

Mehdi Vahidi is a M.Sc. student in structural engineering, university of Tehran, Iran. He is currently a research assistant in research center of school of civil engineering, University of Tehran. His research interests are in the areas of wave propagation, nonlinear analysis and seismic behavior of structures, mehdi.vahidi@ut.ac.ir.